FULL PAPER

Dalton
www.rsc.org/dalton

The synthesis, structure and ethene polymerisation catalysis of mono(salicylaldiminato) titanium and zirconium complexes†

Dale A. Pennington,[a] William Clegg,[b] Simon J. Coles,[c] Ross W. Harrington,[b] Michael B. Hursthouse,[c] David L. Hughes,[a] Mark E. Light,[c] Mark Schormann,[a] Manfred Bochmann[a] and Simon J. Lancaster*[a]

[a] *Wolfson Materials and Catalysis Centre, School of Chemical Sciences and Pharmacy, University of East Anglia, Norwich, UK NR4 7TJ. E-mail: S.Lancaster@uea.ac.uk; Fax: 44 1603 592009; Tel: 44 1603 592009*

[b] *School of Natural Sciences (Chemistry), University of Newcastle, Newcastle upon Tyne, UK NE1 7RU*

[c] *School of Chemistry, University of Southampton, Highfield, Southampton, UK SO17 1BJ*

Received 14th September 2004, Accepted 26th November 2004
First published as an Advance Article on the web 4th January 2005

The silyl ethers 3-Bu^t-2-(OSiMe$_3$)C$_6$H$_3$CH=NR (**2a–e**) have been prepared by deprotonation of the known iminophenols (**1a–e**) and treatment with SiClMe$_3$ (**a**, R = C$_6$H$_5$; **b**, R = 2,6-Pr$^i{}_2$C$_6$H$_3$; **c**, R = 2,4,6-Me$_3$C$_6$H$_2$; **d**, R = 2-C$_6$H$_5$C$_6$H$_4$; **e**, R = C$_6$F$_5$). **2a–c** react with TiCl$_4$ in hydrocarbon solvents to give the binuclear complexes [Ti{3-Bu^t-2-(O)C$_6$H$_3$CH=N(R)}Cl(μ-Cl$_3$)TiCl$_3$] (**3a–c**). The pentafluorophenyl species **2e** reacts with TiCl$_4$ to give the known complex Ti{3-Bu^t-2-(O)C$_6$H$_3$CH=N(R)}$_2$Cl$_2$. The mononuclear five-coordinate complex, Ti{3-Bu^t-2-(O)C$_6$H$_3$CH=N(2,4,6-Me$_3$C$_6$H$_2$)}Cl$_3$ (**4c**), was isolated after repeated recrystallisation of **3c**. Performing the dehalosilylation reaction in the presence of tetrahydrofuran yields the octahedral, mononuclear complexes Ti{3-Bu^t-2-(O)C$_6$H$_3$CH=N(R)}Cl$_3$(THF) (**5a–e**). The reaction with ZrCl$_4$(THF)$_2$ proceeds similarly to give complexes Zr{3-Bu^t-2-(O)-C$_6$H$_3$CH=N(R)}Cl$_3$(THF) (**6b–e**). The crystal structures of **3b**, **4c**, **5a**, **5c**, **5e**, **6b**, **6d**, **6e** and the salicylaldehyde titanium complex Ti{3-Bu^t-2-(O)C$_6$H$_3$CH=O}Cl$_3$(THF) (**7**) have been determined. Activation of complexes **5a–e** and **6b–e** with MAO in an ethene saturated toluene solution gives polyethylene with at best high activity depending on the imine substituent.

Introduction

The ongoing search for new non-metallocene 1-alkene polymerisation catalysts has contributed to intense academic and industrial interest in transition metal coordination chemistry.[1] To date a great many examples of group 4 metal complexes with either two anionic bidentate ancillary ligands or a single dianionic tetradentate ligand have been prepared and tested as catalysts.[2,3] These essentially octahedral compounds offer significant steric protection to the metal centre and their catalytic behaviour is often compared to the metallocenes. However, despite the well documented differences in catalytic behaviour between metallocenes and the much more open mono(cyclopentadienyl) complexes (**I**, Chart 1)[4] there are relatively few examples of synthetic and catalytic studies of mono(bidentate anionic ligand) complexes of the group 4 metals. Important examples include amidinates (**II**),[5] guadinates (**III**)[6] and β-diketiminates (**IV**).[7]

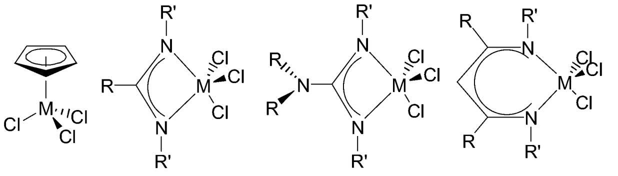

I **II** **III** **IV**

Chart 1

Transition metal complexes of the monoanionic bidentate N,O chelate salicylaldiminato (iminophenolato) ligands have attracted considerable attention since the discovery of highly active,[8] and living[9] bis(salicylaldiminato) group 4 (**V**, Chart 2), mono(salicylaldiminato) chromium[10] and neutral nickel (**VI**)[11] catalysts for the polymerisation of ethene. We recently reported mixed salicylaldiminato cyclopentadienyl complexes of titanium and zirconium (**VII**).[12] The activity of all these pre-catalysts is highly dependent on the nature of the substituents in the *ortho*-position on the phenoxy ring and on the imine nitrogen. We report here the synthesis, structure and stability of a series of mono(salicylaldiminato) complexes of titanium and zirconium intended as precursors to mixed ligand complexes.[13] Our preliminary results on titanium complexes have been communicated.[14] The use of these new complexes as pre-catalysts for ethene polymerisation is described.

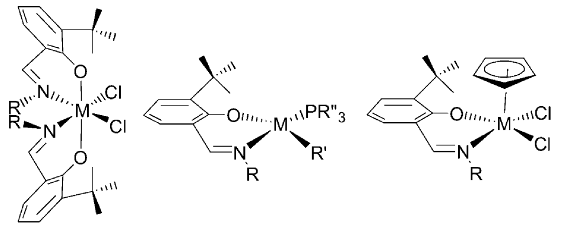

V **VI** **VII**

Chart 2

Results and discussion

Syntheses of complexes

Bis(salicylaldiminato) complexes of the group 4 metals are normally prepared through the reaction of two equivalents of the deprotonated iminophenol with the appropriate metal tetrachloride in tetrahydrofuran solution.[9] Our initial investigations

---

† Electronic supplementary information (ESI) available: Synthetic procedures and full characterisation data. See http://www.rsc.org/suppdata/dt/b4/b414229b/

DOI: 10.1039/b414229b

demonstrated that this approach was not suited to the preparation of mono(salicylaldiminato) complexes. Even the reaction between our most hindered Li{3-Bu^t-2-(O)$C_6H_3CH{=}N$(2,6-$Pr^i_2C_6H_3$)} reagent and $TiCl_4$ was far from selective and led only to an intractable mixture of products.

The requirement for a milder and more selective method to introduce salicylaldiminato ligands led to an examination of the widely employed dehalosilylation route.[15] A series of silyl ethers, 3-Bu^t-2-($OSiMe_3$)$C_6H_3CH{=}NR$ (**2a–e**), was prepared by deprotonation of the known iminophenols (**1a–e**) and treatment with $SiClMe_3$ (Scheme 1). It proved necessary to heat the tetrahydrofuran solution of lithium salt and chlorotrimethylsilane under reflux for several hours to ensure good conversion to the silyl ether.

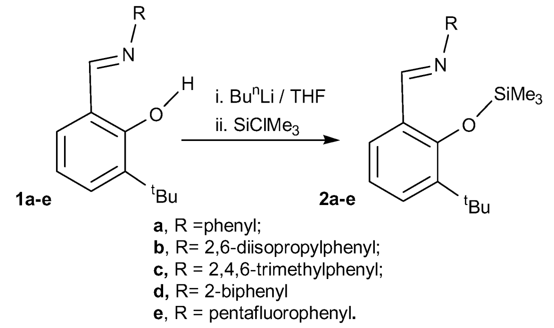

Scheme 1

Treating $ZrCl_4$ with the bulky 2,6-diisopropyl substituted derivative **2b** in dichloromethane solution was not selective and led to a mixture of products including Zr{3-Bu^t-2-(O)$C_6H_3CH{=}N$(2,6-$Pr^i_2C_6H_3$}$_2Cl_2$, which was identified by comparison to the reported NMR data.[8a] In contrast, reacting **2a–c** with $TiCl_4$ in light petroleum solution led to the slow precipitation of dark red solids (**3a–c**). Identical products were obtained in good yield after heating a toluene solution under reflux overnight (Scheme 2). **3a–c** were readily identified by ^1H NMR as the products of a dehalosilylation reaction yielding salicylaldiminato complexes. However, the elemental analyses afforded a N : Cl ratio of 1 : 7 and were consistent with the composition LTi_2Cl_7, not the expected $LTiCl_3$. The nature of the association with the second equivalent of $TiCl_4$ was revealed by determining the crystal structure of **3b** (Fig. 1, for selected bond lengths and angles see Table 1). **3b** is a binuclear complex in which the two titanium centres are bridged by three chloride ligands. The titanium atoms are both six-coordinate with distorted octahedral geometries. One metal centre is bonded to six chloride ligands, the other to four chlorides and the bidentate salicylaldiminato ligand.[14] Complexes **3a** and **3c** are formulated as binuclear complexes analogous to **3b** on the basis of NMR and elemental analysis data.[16] There are few precedents for structures such as **3b**, in which the titanium centre is surrounded only by an octahedron of chloride ligands. The neutral tetranuclear complex {$Cl_3Ti(\mu\text{-}Cl)_3Ti(NPPh_3)$}$_2$($\mu$-Cl)$_2$ (**VIII**, Chart 3) contains titanium with a similar octahedral chloride ligand coordination environment to **3b**; the terminal Ti–Cl bond lengths are similar (2.189–2.213) but the bridging Ti–Cl bond lengths cover a greater range (2.399–2.614).[17] The structure of the $[Ti_2Cl_9]^-$ anion (**IX**), in which both titanium centres have an octahedral face-sharing geometry, has been reported and both the terminal (2.197–2.225 Å) and bridging Ti–Cl (2.480–2.556 Å) bond lengths are very similar to those observed for **3b**.[18]

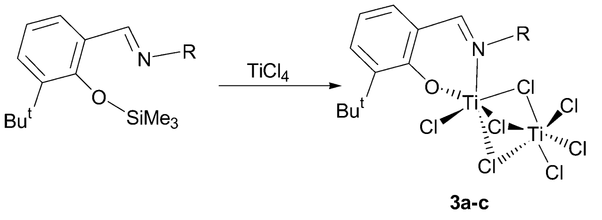

Scheme 2

Table 1 Molecular dimensions for complex **3b**; bond lengths (Å), angles (°), esds are in parentheses

Ti(1)–O(1)	1.7843(16)	Ti(1)–Cl(5)	2.4336(7)
Ti(1)–N(2)	2.138(2)	Ti(1)–Cl(6)	2.4091(7)
Ti(1)–Cl(3)	2.1987(10)	Ti(1)–Cl(4)	2.4907(10)
O(1)–Ti(1)–N(2)	84.76(7)	N(2)–Ti(1)–Cl(4)	87.43(6)
O(1)–Ti(1)–Cl(3)	102.52(6)	Cl(3)–Ti(1)–Cl(5)	93.98(3)
O(1)–Ti(1)–Cl(5)	163.22(6)	Cl(3)–Ti(1)–Cl(6)	92.97(3)
O(1)–Ti(1)–Cl(6)	100.33(5)	Cl(3)–Ti(1)–Cl(4)	171.28(3)
O(1)–Ti(1)–Cl(4)	84.37(6)	Cl(6)–Ti(1)–Cl(5)	81.62(2)
N(2)–Ti(1)–Cl(3)	98.44(6)	Cl(5)–Ti(1)–Cl(4)	79.51(2)
N(2)–Ti(1)–Cl(5)	89.87(5)	Cl(6)–Ti(1)–Cl(4)	80.40(3)
N(2)–Ti(1)–Cl(6)	166.23(6)		
O(1)–C(1)	1.352(3)	C(20)–N(2)	1.285(3)
C(1)–C(2)	1.409(3)	N(2)–C(21)	1.466(3)
C(2)–C(20)	1.436(3)		
C(1)–O(1)–Ti(1)	135.86(14)	C(20)–N(2)–Ti(1)	120.85(15)
O(1)–C(1)–C(2)	116.1(2)	C(21)–N(2)–Ti(1)	124.29(15)
C(1)–C(2)–C(20)	122.1(2)	C(20)–N(2)–C(21)	114.85(19)
N(2)–C(20)–C(2)	128.1(2)		
Ti(1) · · · Ti(2)	3.3578(7)		
Ti(2)–Cl(4)	2.4618(9)	Ti(2)–Cl(7)	2.2106(10)
Ti(2)–Cl(5)	2.5417(7)	Ti(2)–Cl(8)	2.1845(9)
Ti(2)–Cl(6)	2.5381(9)	Ti(2)–Cl(9)	2.1971(7)
Cl(4)–Ti(2)–Cl(5)	78.00(3)	Cl(9)–Ti(2)–Cl(5)	164.20(3)
Cl(4)–Ti(2)–Cl(6)	78.48(3)	Cl(7)–Ti(2)–Cl(6)	89.87(4)
Cl(7)–Ti(2)–Cl(4)	165.61(3)	Cl(8)–Ti(2)–Cl(6)	164.38(3)
Cl(8)–Ti(2)–Cl(4)	90.71(3)	Cl(9)–Ti(2)–Cl(6)	90.69(3)
Cl(9)–Ti(2)–Cl(4)	89.89(3)	Cl(8)–Ti(2)–Cl(7)	98.90(4)
Cl(6)–Ti(2)–Cl(5)	77.08(2)	Cl(9)–Ti(2)–Cl(7)	98.76(3)
Cl(7)–Ti(2)–Cl(5)	91.27(3)	Cl(8)–Ti(2)–Cl(9)	100.63(4)
Cl(8)–Ti(2)–Cl(5)	89.75(3)		
Ti(2)–Cl(4)–Ti(1)	85.38(3)	Ti(1)–Cl(6)–Ti(2)	85.45(3)
Ti(1)–Cl(5)–Ti(2)	84.86(2)		

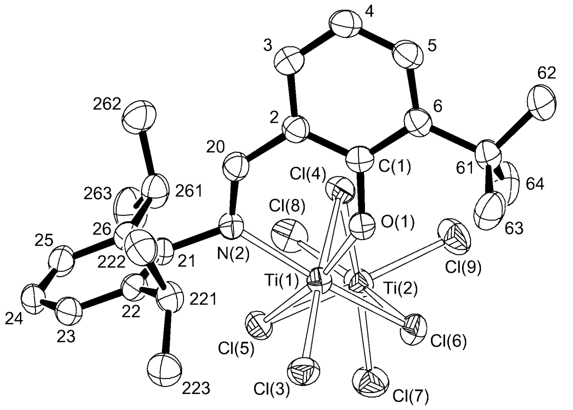

Fig. 1 Structure of **3b** with displacement ellipsoids at the 50% probability level; H atoms are omitted for clarity, C atoms are labeled by number only.

The stability of the binuclear complexes **3** towards further reaction is remarkable; **3a–c** do not react with a second equivalent of ligand even after heating under reflux for two days in toluene solution. Despite this, formation of these LTi_2Cl_7 structures does appear to be specific to simple aryl-substituted salicylaldiminato ligands. Lapido has shown that alkyl substituted analogues react in a 1 : 1 fashion to form monomeric $LTiCl_3$ (for example **X**) or dimeric $L_2Ti_2Cl_6$ complexes (for example **XI**) with less bulky substituents.[14b] The reaction of the electron-poor ligand precursor **2e** with $TiCl_4$ proceeded quite differently, leading not

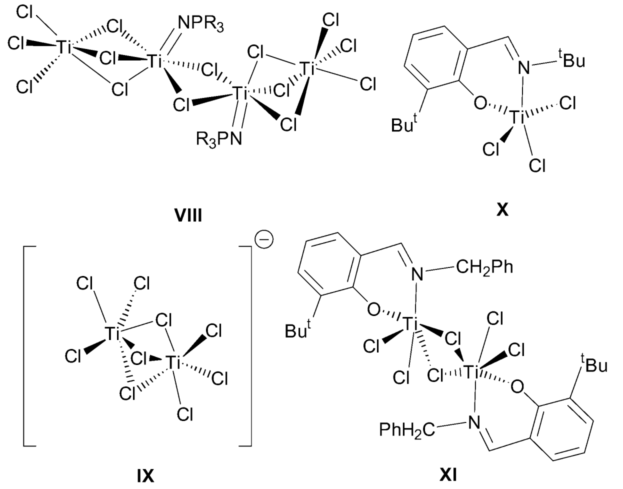

Chart 3

Table 2 Molecular dimensions for complex **4c**; bond lengths (Å), angles (°), esds are in parentheses

Ti(1)–O(1)	1.8152(13)	Ti(1)–Cl(3)	2.2327(6)
Ti(1)–N(1)	2.1478(14)	Ti(1)–Cl(2)	2.2769(6)
		Ti(1)–Cl(1)	2.2327(6)
O(1)–Ti(1)–N(1)	81.10(5)	Cl(2)–Ti(1)–N(1)	86.62(4)
Cl(3)–Ti(1)–O(1)	92.79(5)	Cl(1)–Ti(1)–N(1)	128.80(5)
Cl(2)–Ti(1)–O(1)	167.49(4)	Cl(2)–Ti(1)–Cl(3)	94.91(2)
Cl(1)–Ti(1)–O(1)	92.45(5)	Cl(1)–Ti(1)–Cl(3)	113.93(3)
Cl(3)–Ti(1)–N(1)	117.07(5)	Cl(1)–Ti(1)–Cl(2)	93.42(2)
O(1)–C(16)	1.331(2)	N(1)–C(10)	1.305(2)
C(11)–C(16)	1.406(2)	N(1)–C(1)	1.459(2)
C(10)–C(11)	1.428(2)		
Ti(1)–O(1)–C(16)	147.61(11)	Ti(1)–N(1)–C(10)	125.39(12)
O(1)–C(16)–C(11)	115.65(15)	Ti(1)–N(1)–C(1)	121.90(10)
C(10)–C(11)–C(16)	121.33(15)	C(1)–N(1)–C(10)	112.60(14)
N(1)–C(10)–C(11)	128.27(15)		

to a binuclear species but to the bis(salicylaldiminato) complex Ti{3-Bu^t-2-(O)C_6H_3CH=N(C_6F_5}$_2Cl_2$, which was identified by crystallography and comparison to the known structure.[9e]

The initial product of the reaction between **2c** and $TiCl_4$ was the poorly crystalline binuclear complex **3c**. Repeated recrystallisation of **3c** afforded single crystals of a new complex **4c**, which were very small but of sufficient quality for a structure determination (Fig. 2, for selected bond lengths and angles see Table 2). The monomeric solid state structure of **4c** contrasts with the chloride-bridged dimeric structures determined for mono(amidinate)[5b] and mono(guanidinate) titanium trichlorides[6] and the benzyl substituted mono(salicylaldiminato) complex **XI**. It does however, resemble the trigonal bipyramidal structure of the *tert*-butyl substituted mono(salicylaldiminato) complex **X**. The most significant difference between **X** and **4c** sees the imine nitrogen, rather than the phenoxide oxygen, in an axial site.[19]

The mononuclear complex **4c** is the result of the loss of one equivalent of $TiCl_4$ from the binuclear precursor **3c**. **4c** is not accessible through direct reaction of $TiCl_4$ with **2c**. As yet we have not been able to develop a convenient synthesis of **4c** or its analogues, despite its evident stability and the facile synthesis of the closely related complex, **X**.

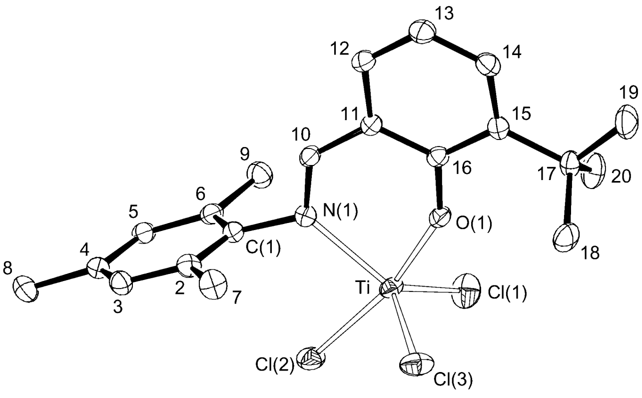

Fig. 2 Structure of **4c** with displacement ellipsoids at the 50% probability level.

The pattern of reactivity between the base-free titanium and zirconium tetrachlorides and the silyl ethers reported here is reminiscent of that observed for trimethylsilylcyclopentadienes. For the cyclopentadienyl zirconium system Livinghouse and Lund demonstrated that the reactivity of the metal centre could be moderated by the addition of a basic donor.[15b] When the tetrahydrofuran adduct $TiCl_4(THF)_2$ was treated with the silyl ethers **2** in dichloromethane solution the reaction proceeded slowly and smoothly to yield dark red six-coordinate mono(salicylaldiminato) complexes Ti{3-Bu^t-2-(O)C_6H_3CH=NR}Cl_3(THF) (**5a–e**) (Scheme 3). In each case satisfactory elemental analyses were obtained with N : Cl ratios of 1 : 3. The ^1H NMR spectra clearly indicated that a dehalosilylation reaction and complex formation had taken place. Identical THF adducts could also be obtained through treating solutions of **3a–c** or **4c** with excess THF. Three of the five titanium complexes prepared, **5a** (Fig. 3), **5c** (Fig. 4) and **5e** (Fig. 5) have been crystallographically characterised (selected bond lengths and angles are collected in Table 3).

5a adopts an essentially octahedral geometry. The three chloride ligands are meridionally arranged. The two O ligating atoms are mutually *trans*; in this respect the geometry is similar to the bis(salicylaldiminato) titanium complex Ti{3-Bu^t-2-(O)C_6H_3CH=NPh}$_2Cl_2$ (O–Ti–O = 171.6°).[9c] Complex **5c** also adopts a distorted octahedral coordination pattern about the Ti atom, but now the three Cl atoms are facially arranged and both the phenoxy and THF ligating O atoms are *trans* to chlorides. Complex **5e** has a similar distorted octahedral geometry and relative arrangement of ligands to those in **5c**, the greatest difference being in the orientation of the THF ligand. For complexes **5a**, **5c** and **5e** the metal–ligand bond lengths to the salicylaldiminato and chloride ligands are close to those observed in Ti{3-Bu^t-2-(O)C_6H_3CH=NPh}$_2Cl_2$[9c] and TiCp{3-Bu^t-2-(O)C_6H_3CH=N(2,4,6-$Me_3C_6H_2$}Cl_2.[12] Not surprisingly, the

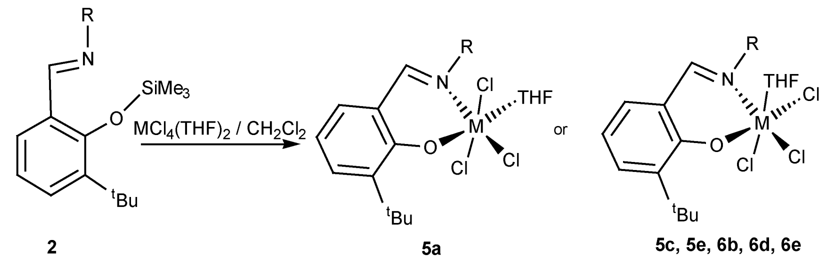

5, M = Ti; **6**, M = Zr.
a, R =phenyl;
b, R= 2,6-diisopropylphenyl;
c, R = 2,4,6-trimethylphenyl;
d, R= 2-biphenyl
e, R = pentafluorophenyl.

Scheme 3

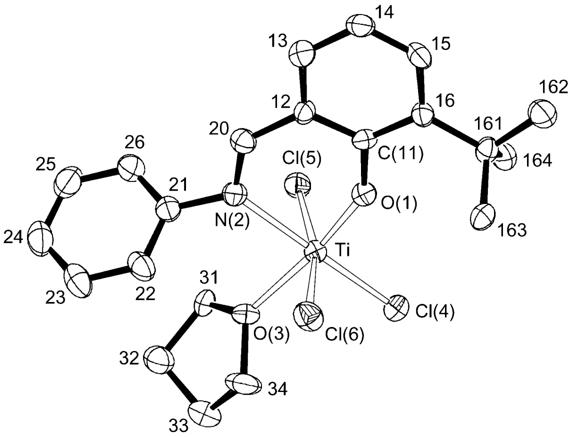

Fig. 3 Structure of **5a** with displacement ellipsoids at the 50% probability level.

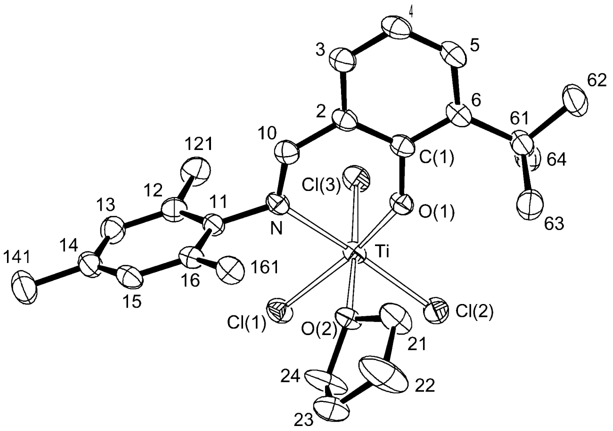

Fig. 4 Structure of **5c** with displacement ellipsoids at the 50% probability level.

terminal Ti–Cl distances are longer than those seen in **4c**, which in turn are longer than those of **3b**. This reflects the expected decrease in Lewis acidity **3** > **4** > **5**, moving from the binuclear complex to the THF adduct. The related mono(amidinate) titanium complex $Ti\{PhC(NSiMe_3)_2\}Cl_3(THF)$ has the facial arrangement of chloride ligands seen for **5c** and **5e** rather than the meridional pattern of **5a**.[5b]

In contrast to the non-selective reaction with base-free $ZrCl_4$, $ZrCl_4(THF)_2$ underwent clean dehalosilylation with the silyl ethers **2b–d** in dichloromethane solution to yield the yellow products (**6b–e**) (Scheme 3). The ^1H NMR spectra exhibited the expected pattern of resonances for a bidentate ligand and one equivalent of THF. The room-temperature NMR spectra of **6b**, **6e** (and their titanium analogues **5b** and **5e**) gave two resonances for the *ortho*-substituents on the imine phenyl ring, indicating a significant steric hindrance to rotation about the N–C bond. The elemental analyses were consistent with the expected compositions. Confirmation that we had successfully prepared the first examples of mono(salicylaldiminato) zirconium complexes $Zr\{3\text{-}Bu^t\text{-}2\text{-}(O)C_6H_3CH{=}NR\}Cl_3(THF)$ (**6b–e**) was provided by the crystal structure determinations of **6b** (Fig. 6), **6d** (Fig. 7) and **6e** (Fig. 8). Selected bond lengths and angles for these complexes are collected in Table 4.

Structurally the zirconium complexes, exemplified in **6b**, **6d**, and **6e**, are similar to **5c** and **5e**, with distorted octahedral coordination and a *fac* arrangement of the three Cl ligands. However, as the steric bulk of the Ar group increases, from **6b** to **6d**, the distortion about the metal atom increases – this is

Table 3 Molecular dimensions for complexes **5a**, **5c** and **5e**; bond lengths (Å), angles (°), esds are in parentheses

5a		5c		5e	
Ti–O(1)	1.791(5)	Ti–O(1)	1.8328(15)	O(1)–Ti(1)	1.8191(18)
Ti–N(2)	2.240(6)	Ti–N	2.2558(17)	N(1)–Ti(1)	2.248(2)
Ti–Cl(6)	2.327(2)	Ti–O(2)	2.1669(14)	O(2)–Ti(1)	2.0981(19)
Ti–O(3)	2.146(5)	Ti–Cl(1)	2.3196(9)	Cl(1)–Ti(1)	2.3169(8)
Ti–Cl(4)	2.281(2)	Ti–Cl(2)	2.2943(9)	Cl(2)–Ti(1)	2.2587(8)
Ti–Cl(5)	2.342(2)	Ti–Cl(3)	2.2914(8)	Cl(3)–Ti(1)	2.2768(8)
O(1)–Ti–N(2)	83.1(2)	O(1)–Ti–N	81.27(6)	O(1)–Ti(1)–N(1)	80.41(8)
O(1)–Ti–Cl(6)	91.85(15)	O(1)–Ti–O(2)	88.40(6)	O(1)–Ti(1)–O(2)	86.04(8)
O(1)–Ti–O(3)	171.76(19)	O(1)–Ti–Cl(1)	168.64(5)	O(1)–Ti(1)–Cl(1)	165.45(6)
O(1)–Ti–Cl(4)	98.00(16)	O(1)–Ti–Cl(2)	94.97(5)	O(1)–Ti(1)–Cl(2)	97.06(6)
O(1)–Ti–Cl(5)	94.36(15)	O(1)–Ti–Cl(3)	90.72(5)	O(1)–Ti(1)–Cl(3)	92.40(6)
N(2)–Ti–Cl(6)	87.14(16)	O(2)–Ti–N	84.55(6)	O(2)–Ti(1)–N(1)	86.59(8)
O(3)–Ti–N(2)	88.8(2)	N–Ti–Cl(1)	87.99(5)	N(1)–Ti(1)–Cl(1)	86.28(6)
N(2)–Ti–Cl(4)	176.72(18)	N–Ti–Cl(2)	169.86(4)	N(1)–Ti(1)–Cl(2)	174.73(6)
N(2)–Ti–Cl(5)	82.48(16)	N–Ti–Cl(3)	91.73(5)	N(1)–Ti(1)–Cl(3)	88.80(6)
O(3)–Ti–Cl(6)	86.70(13)	O(2)–Ti–Cl(1)	86.89(5)	O(2)–Ti(1)–Cl(1)	87.36(6)
Cl(4)–Ti–Cl(6)	95.91(8)	O(2)–Ti–Cl(2)	85.95(5)	O(2)–Ti(1)–Cl(2)	88.63(5)
Cl(6)–Ti–Cl(5)	167.17(9)	O(2)–Ti–Cl(3)	176.26(4)	O(2)–Ti(1)–Cl(3)	175.31(6)
O(3)–Ti–Cl(4)	90.21(14)	Cl(2)–Ti–Cl(1)	95.00(3)	Cl(2)–Ti(1)–Cl(1)	95.73(3)
O(3)–Ti–Cl(5)	85.55(13)	Cl(3)–Ti–Cl(1)	93.32(4)	Cl(3)–Ti(1)–Cl(1)	93.14(3)
Cl(4)–Ti–Cl(5)	94.34(8)	Cl(3)–Ti–Cl(2)	97.75(3)	Cl(2)–Ti(1)–Cl(3)	95.95(3)
O(1)–C(11)	1.371(7)	O(1)–C(1)	1.356(2)	C(13)–O(1)	1.340(3)
C(11)–C(12)	1.403(9)	C(1)–C(2)	1.408(3)	C(8)–C(13)	1.411(4)
C(12)–C(20)	1.465(9)	C(2)–C(10)	1.452(3)	C(7)–C(8)	1.430(4)
N(2)–C(20)	1.296(8)	N–C(10)	1.305(3)	C(7)–N(1)	1.297(3)
N(2)–C(21)	1.448(10)	N–C(11)	1.463(2)	C(1)–N(1)	1.437(3)
C(11)–O(1)–Ti	146.1(5)	C(1)–O(1)–Ti	140.64(13)	C(13)–O(1)–Ti(1)	143.21(17)
O(1)–C(11)–C(12)	116.4(6)	O(1)–C(1)–C(2)	116.83(17)	O(1)–C(13)–C(8)	116.8(2)
C(11)–C(12)–C(20)	123.4(6)	C(1)–C(2)–C(10)	122.38(18)	C(13)–C(8)–C(7)	122.5(2)
N(2)–C(20)–C(12)	127.7(7)	N–C(10)–C(2)	127.82(19)	N(1)–C(7)–C(8)	127.2(2)
C(20)–N(2)–Ti	123.0(5)	C(10)–N–Ti	122.19(13)	C(7)–N(1)–Ti(1)	122.87(17)
C(21)–N(2)–Ti	121.2(4)	C(11)–N–Ti	124.13(12)	C(1)–N(1)–Ti(1)	122.68(16)
C(20)–N(2)–C(21)	115.2(6)	C(10)–N–C(11)	113.68(16)	C(7)–N(1)–C(1)	113.4(2)

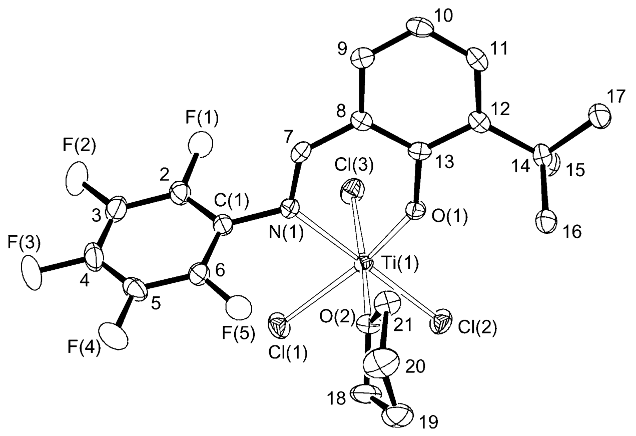

Fig. 5 Structure of **5e** with displacement ellipsoids at the 50% probability level.

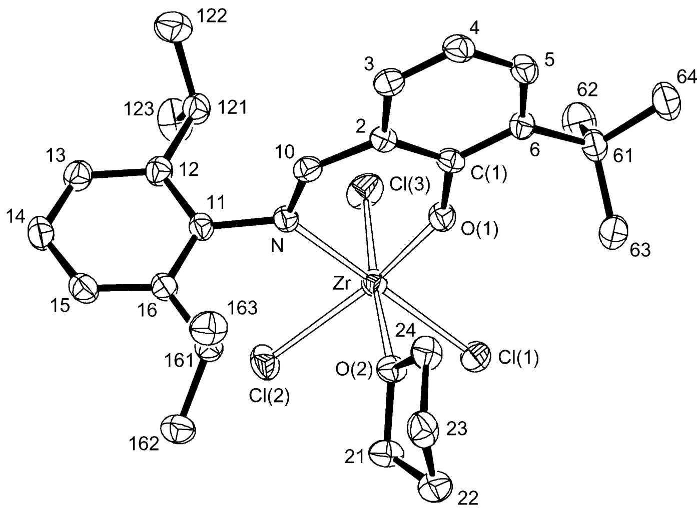

Fig. 6 Structure of **6b** displacement ellipsoids at the 50% probability level.

observed in the dimensions, *e.g.* the *trans* O(1)–Zr–Cl angles at 161.72(4), 155.99(8) and 161.50(5)° in **6b**, **6d** and **6e**. In **5e** and **6e** there is a slight shortening of the M–Cl bond *trans* to the perfluorophenyl substituted imine donor, relative both to the *cis* M–Cl bonds and the *trans* M–Cl bonds found in the other derivatives.

Careful inspection of the structure of **6e** reveals a close contact (2.59 Å) between a hydrogen atom on the 2-position of the THF ligand and an *ortho*-fluorine (the closest contact in **5e** is 2.70 Å). This distance is essentially the sum of the van der Waals radii and this steric interaction along with one to Cl(3) may make a significant contribution to the resistance to rotation about the NC_6F_5 bond. Shorter, stronger interactions between β-H atoms and the *ortho*-fluorines of C_6F_5 substituents have been proposed to account for the ability of the bis(salicylaldiminato) complexes to promote living 1-alkene polymerisation.[9e]

The zirconium–ligand bond distances in these complexes show little variation and are comparable with those found in the bis(salicylaldiminato) complexes $Zr\{3\text{-}Bu^t\text{-}2\text{-}(O)C_6H_3CH{=}NC_6H_5\}Cl_2$[8a] and $Zr\{3\text{-}Bu^t\text{-}2\text{-}(O)C_6H_3CH{=}N(2,4,6\text{-}Me_3C_6H_2)\}Cl_2$.[12] Structurally they resemble the mono(guanidinato)zirconium complex $Zr\{(Pr^iNH)C(NPr^i)_2\}Cl_3(THF)$, which also has a distorted octahedral coordination sphere completed by a THF donor and a *fac* arrangement of the three chloride ligands.[20]

Table 4 Molecular dimensions for complexes **6b**, **6d** and **6e**; bond lengths (Å), angles (°), esds are in parentheses

6b		**6d**		**6e**	
Zr–O(1)	1.9512(17)	O(1)–Zr(1)	1.953(2)	O(1)–Zr(1)	1.9561(14)
Zr–N	2.3934(17)	N(1)–Zr(1)	2.371(3)	N(1)–Zr(1)	2.3857(17)
Zr–O(2)	2.2596(15)	O(2)–Zr(1)	2.244(2)	O(2)–Zr(1)	2.2187(15)
Zr–Cl(2)	2.4303(8)	Cl(3)–Zr(1)	2.4306(9)	Cl(3)–Zr(1)	2.4415(5)
Zr–Cl(1)	2.4223(7)	Cl(1)–Zr(1)	2.4350(9)	Cl(1)–Zr(1)	2.4049(6)
Zr–Cl(3)	2.3974(7)	Cl(2)–Zr(1)	2.4032(9)	Cl(2)–Zr(1)	2.4157(5)
O(1)–Zr–N	77.19(6)	O(1)–Zr(1)–N(1)	76.39(10)	O(1)–Zr(1)–N(1)	76.68(6)
O(1)–Zr–O(2)	84.73(6)	O(1)–Zr(1)–O(2)	82.05(10)	O(1)–Zr(1)–O(2)	84.41(6)
O(1)–Zr–Cl(2)	161.72(4)	O(1)–Zr(1)–Cl(3)	155.99(8)	O(1)–Zr(1)–Cl(3)	161.50(5)
O(1)–Zr–Cl(1)	96.46(4)	O(1)–Zr(1)–Cl(1)	97.77(7)	O(1)–Zr(1)–Cl(1)	98.04(5)
O(1)–Zr–Cl(3)	93.34(5)	O(1)–Zr(1)–Cl(2)	99.03(8)	O(1)–Zr(1)–Cl(2)	93.65(4)
O(2)–Zr–N	86.20(5)	O(2)–Zr(1)–N(1)	93.17(10)	O(2)–Zr(1)–N(1)	85.49(6)
N–Zr–Cl(2)	86.44(5)	N(1)–Zr(1)–Cl(3)	85.86(7)	N(1)–Zr(1)–Cl(3)	85.92(4)
N–Zr–Cl(1)	167.99(5)	N(1)–Zr(1)–Cl(1)	174.13(8)	N(1)–Zr(1)–Cl(1)	171.10(5)
N–Zr–Cl(3)	96.68(4)	N(1)–Zr(1)–Cl(2)	89.26(7)	N(1)–Zr(1)–Cl(2)	92.81(4)
O(2)–Zr–Cl(2)	86.15(5)	O(2)–Zr(1)–Cl(3)	82.94(7)	O(2)–Zr(1)–Cl(3)	88.06(4)
O(2)–Zr–Cl(1)	83.05(4)	O(2)–Zr(1)–Cl(1)	85.36(7)	O(2)–Zr(1)–Cl(1)	86.88(4)
O(2)–Zr–Cl(3)	176.11(4)	O(2)–Zr(1)–Cl(2)	177.52(7)	O(2)–Zr(1)–Cl(2)	177.67(4)
Cl(1)–Zr–Cl(2)	98.13(2)	Cl(3)–Zr(1)–Cl(1)	99.58(3)	Cl(1)–Zr(1)–Cl(3)	98.40(2)
Cl(3)–Zr–Cl(2)	96.62(3)	Cl(2)–Zr(1)–Cl(3)	96.74(4)	Cl(2)–Zr(1)–Cl(3)	93.42(2)
Cl(3)–Zr–Cl(1)	93.83(2)	Cl(2)–Zr(1)–Cl(1)	92.27(3)	Cl(1)–Zr(1)–Cl(2)	94.68(2)
O(1)–C(1)	1.350(2)	C(1)–O(1)	1.340(4)	C(13)–O(1)	1.343(2)
C(1)–C(2)	1.408(3)	C(1)–C(10)	1.406(5)	C(8)–C(13)	1.408(3)
C(2)–C(10)	1.438(3)	C(10)–C(11)	1.444(5)	C(7)–C(8)	1.436(3)
C(10)–N	1.308(3)	C(11)–N(1)	1.298(5)	C(7)–N(1)	1.309(3)
N–C(11)	1.470(3)	C(12)–N(1)	1.459(4)	C(1)–N(1)	1.437(3)
C(1)–O(1)–Zr	149.14(14)	C(1)–O(1)–Zr(1)	148.1(2)	C(13)–O(1)–Zr(1)	147.31(14)
O(1)–C(1)–C(2)	116.4(2)	O(1)–C(1)–C(10)	117.5(3)	O(1)–C(13)–C(8)	117.16(18)
C(1)–C(2)–C(10)	123.40(19)	C(1)–C(10)–C(11)	122.6(3)	C(13)–C(8)–C(7)	123.34(19)
N–C(10)–C(2)	130.05(19)	N(1)–C(11)–C(10)	127.9(3)	N(1)–C(7)–C(8)	128.6(2)
C(10)–N–Zr	123.46(15)	C(11)–N(1)–Zr(1)	125.9(2)	C(7)–N(1)–Zr(1)	123.99(14)
C(11)–N–Zr	124.33(13)	C(12)–N(1)–Zr(1)	118.7(2)	C(1)–N(1)–Zr(1)	123.52(13)
C(10)–N–C(11)	112.07(17)	C(11)–N(1)–C(12)	114.6(3)	C(7)–N(1)–C(1)	111.98(18)

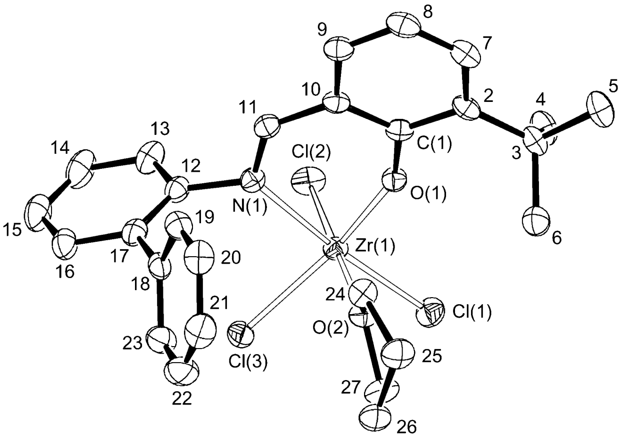

Fig. 7 Structure of **6d** with displacement ellipsoids at the 50% probability level.

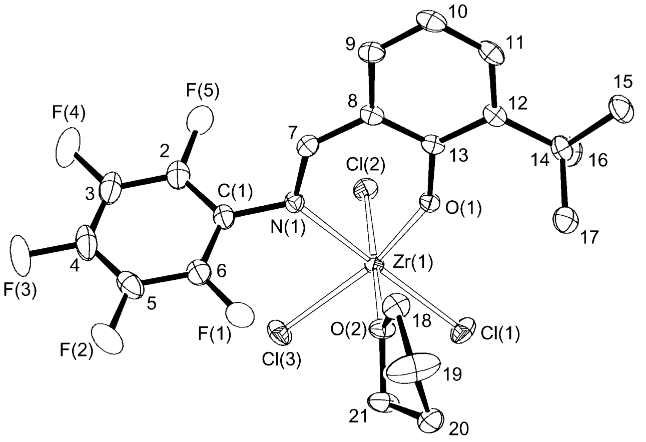

Fig. 8 Structure of **6e** with displacement ellipsoids at the 50% probability level.

It appears that in octahedral mono(salicylaldiminato) complexes bulkier NAr groups, for example those in **5c**, **5e**, **6b**, **6d** and **6e**, enforce a facial arrangement of the chloride ligands and *cis* oxygen donors. Where there is less steric encumbrance such as in **5a**, the electronically favourable *trans* oxygen arrangement reminiscent of the bis(ligand) complexes is found.[8a] Further support for this rationalisation is provided by the salicylaldehyde complex Ti$\{$3-Bu^t-2-(O)C$_6$H$_3$CH=O$\}$Cl$_3$(THF) (**7**), which was isolated from the reaction between the silyl ether derivative of the parent aldehyde and TiCl$_4$(THF)$_2$ (Scheme 4). The crystal structure of **7** (Fig. 9, for selected bond lengths and angles see Table 5) is similar to that of **5a**, with the aldehyde replacing the phenylimine donor, leading to mutually *trans* oxygen atoms and meridional chlorides.

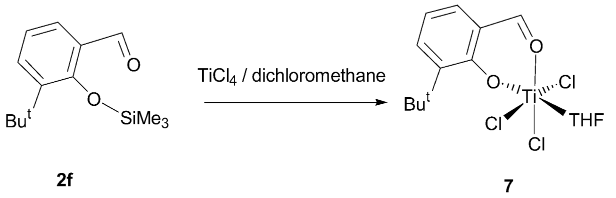

Scheme 4

In the absence of oxygen and moisture all the six-coordinate mononuclear titanium complexes (**5**) are indefinitely stable in aromatic and halocarbon solution. In contrast, the stability of the zirconium complexes (**6**) is dependent on the nature of the imine-substituent. Whereas **6b**, **6c** and **6e** appeared unchanged when dissolved in deuterated dichloromethane or chloroform for spectroscopic characterisation, **6d** underwent partial dissociation, giving rise to resonances for free and coordinated THF and two sets of ligand signals; presumably one for the THF adduct and one for the THF-free complex. Furthermore, when **6b–6e** were dissolved in toluene and left to stand for an extended period the formation of colourless precipitates was observed. For **6e** this process was monitored by ^{1}H NMR in d$_8$-toluene solution over a period of several days. The resonances for **6e** slowly decreased in intensity, with a concomitant increase in the intensity of new ligand signals, which by comparison to the literature data were ascribed to formation of the bis(salicylaldiminato) complex Zr$\{$3-Bu^t-2-(O)C$_6$H$_3$CH=N(C$_6$F$_5$)$\}_2$Cl$_2$. We interpret these observations as being consistent with a ligand redistribution pathway that leads to the decomposition of complexes **6** (Scheme 5), the rate of which is dependent on the imine-substituent. Clearly, the stability of these complexes and the identity of any decomposition products has important implications for their use as catalyst precursors.

Table 5 Molecular dimensions for complex **7**; bond lengths (Å), angles (°), esds are in parentheses

O(2)–Ti(1)	1.825(9)	O(3)–Ti(1)	2.100(9)
O(1)–Ti(1)	2.094(9)	Cl(3)–Ti(1)	2.256(4)
Cl(1)–Ti(1)	2.312(4)	Cl(2)–Ti(1)	2.321(4)
O(2)–Ti(1)–O(1)	83.7(4)	O(1)–Ti(1)–Cl(2)	85.9(3)
O(2)–Ti(1)–Cl(1)	89.3(3)	O(3)–Ti(1)–Cl(1)	85.7(3)
O(2)–Ti(1)–O(3)	165.6(4)	Cl(3)–Ti(1)–Cl(1)	94.52(15)
O(2)–Ti(1)–Cl(3)	98.4(3)	Cl(1)–Ti(1)–Cl(2)	168.64(17)
O(2)–Ti(1)–Cl(2)	95.9(3)	O(3)–Ti(1)–Cl(3)	95.4(3)
O(1)–Ti(1)–Cl(1)	84.6(3)	O(3)–Ti(1)–Cl(2)	86.9(3)
O(1)–Ti(1)–O(3)	82.4(4)	Cl(3)–Ti(1)–Cl(2)	94.70(15)
O(1)–Ti(1)–Cl(3)	177.7(3)		
C(7)–O(2)	1.330(16)	C(1)–C(2)	1.431(18)
C(2)–C(7)	1.431(18)	C(1)–O(1)	1.257(15)
C(7)–O(2)–Ti(1)	137.4(8)	O(1)–C(1)–C(2)	126.0(11)
O(2)–C(7)–C(2)	116.6(12)	C(1)–O(1)–Ti(1)	125.7(9)
C(1)–C(2)–C(7)	122.0(11)		

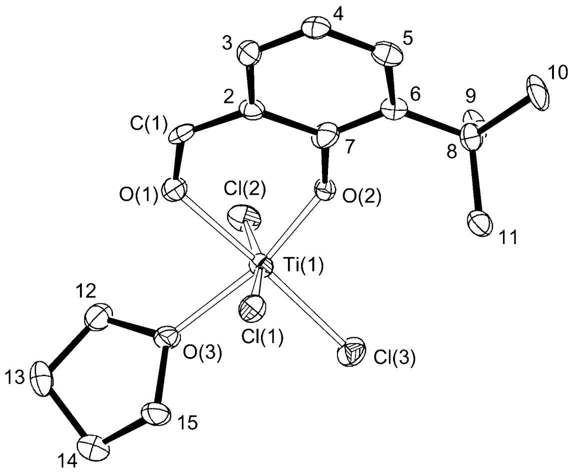

Fig. 9 Structure of **7** with displacement ellipsoids at the 50% probability level.

Polymerisations

The mono(salicylaldiminato) titanium complexes **5a–e** were screened as ethene polymerisation pre-catalysts in combination with MAO (methylaluminoxane). The results are presented in Table 6. The productivity was found to be fairly insensitive to the Al : Ti ratio in the range 200 : 5000, therefore a constant loading of 1000 equivalents was employed for comparison throughout. The highest and most consistent productivities were obtained by pre-mixing the pre-catalyst for two minutes with

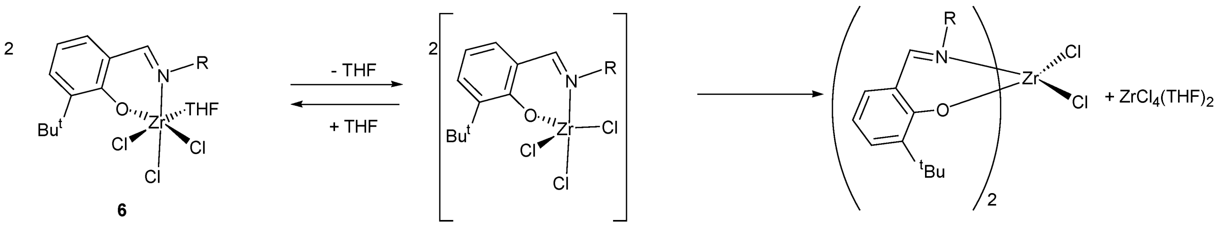

Scheme 5

Table 6 Ethene polymerisation results for the titanium mono(salicylaldiminato) complexes[a]

Run	Complex/μmol	T/°C	t/min	Polymer yield/g	Productivity[b]	M_w	M_n	Polydispersity index
1	**5a** (6)	0	5	0.121	230	235000	140000	1.7
2	**5a** (6)	20	5	0.158	300	271000	148000	1.8
3	**5a** (6)	60	5	0.233	440	171000	73000	2.3
4	**5b** (6)	0	35	0.103	30	513000	8000	mm
5	**5b** (6)	20	35	0.168	50	1120000	7000	mm
6	**5b** (6)	60	35	0.074	20	252000	12000	mm
7	**5c** (6)	0	60	0.020	3	nd	nd	nd
8	**5c** (6)	20	60	0.020	3	nd	nd	nd
9	**5c** (6)	60	60	0.010	1	nd	nd	nd
10	**5d** (6)	0	10	0.055	55	933000	27000	mm
11	**5d** (6)	20	10	0.093	93	1170000	7000	mm
12	**5d** (6)	60	10	0.013	13	209000	4000	mm
13	**5e** (6)	0	5	0.008	16	690000	14000	mm
14	**5e** (6)	20	5	0.026	52	719000	9000	mm
15	**5e** (6)	60	5	0.024	49	883000	1800	mm

[a] In 50 cm^3, 1 bar ethene pressure, 6 mmol MAO. [b] × 10^{-3} g PE {(mol metal) h bar}$^{-1}$. nd = not determined; mm = multimodal.

half of the MAO before injection into the reactor. In no case did the productivity exceed 10^6 g PE {(mol metal) h bar}$^{-1}$ and polymer yields showed an essentially linear dependence on catalyst loading. Therefore we believe the productivity values are an accurate measure of the catalyst system and are not affected by mass transport limitation. For the titanium pre-catalysts **5a–e** we did not observe a strong temperature dependence of productivity. This is possibly the net result of a balance between the competing effects of the increase in propagation rate and decrease in monomer concentration with increasing temperature. The data suggest that the catalyst activation step is facile and that these catalyst systems have a measure of thermal stability across the range 0–60 °C.

The phenyl-substituted complex **5a** was found to give both the highest activity (440 kg PE {(mol metal) h bar}$^{-1}$) at 60 °C and the smallest polydispersity index (*e.g.* 2.3, run 3). Increasing the steric bulk of the imine substituent causes a decrease in productivity but a modest increase in M_w (see runs 6 and 12). The productivity of these bulkier derivatives is in line with that reported for the *tert*-butyl substituted pre-catalyst **X** (30 kg {(mol metal) h bar}$^{-1}$).[14b] While GPC (gel permeation chromatography) data were obtained for runs 4–6 and 10–15, the traces are multimodal and therefore meaningful values for the polydispersity could not be extracted. The implication is that **5b–e** react with MAO to give rise to a number of catalytically active species. We and Fujita have observed similar behaviour with salicylaldiminato derived catalysts before.[12,21,22]

The mono(salicylaldiminato) zirconium complexes **6b–e** were screened as ethene polymerisation pre-catalysts in combination with MAO and the results for **6b**, **6d** and **6e** are presented in Table 7. **6c** displayed very low activity and gave only a trace of polymer under the experimental conditions employed. The catalyst derived from **6e** was the only one to exhibit greater than moderate productivity.

It is tempting to assume that the distinctive catalytic behaviour of **5a**/MAO is indicative of a single-site cationic mono(salicylaldiminato) titanium dialkyl catalyst. However, the multimodal traces for **5b–e** suggest that the true picture may be somewhat more complicated. Zambelli's report of the apparent generation of bis(amidinate) titanium catalysts by the in-situ disproportionation of mono(amidinate) complexes, during propene polymerisation, is a plausible model for the processes that may be at work in our system.[5b] Additional

Table 7 Ethene polymerisation results for zirconium mono(salicylaldiminato) complexes[a]

Run	Complex/μmol	T/°C	t/min	Polymer Yield/g	Productivity[b]	M_w	M_n	Polydispersity index
16	**6b** (6)	0	10	Trace	Very low	nd	nd	nd
17	**6b** (6)	20	10	0.020	17	nd	nd	nd
18	**6b** (6)	60	10	0.019	16	nd	nd	nd
19	**6d** (6)	0	10	0.059	59	nd	nd	nd
20	**6d** (6)	20	10	0.075	75	nd	nd	nd
21	**6d** (6)	60	10	0.035	35	nd	nd	nd
22	**6e** (6)	−20	5	0.293	590	266000	74000	3.6
23	**6e** (6)	0	5	0.342	680	133000	47000	2.8
24	**6e** (6)	20	5	0.534	1100	28000	9500	3
25	**6e** (6)	60	5	0.155	52	9300	2000	4.6

[a] In 50 cm^3, 1 bar ethene pressure, 6 mmol MAO. [b] × 10^{-3} g PE {(mol metal) h bar}$^{-1}$ nd = not determined (insufficient material).

catalytically active species may also be formed through inter- or intra-molecular alkylation of the ligand imine function.[22]

Conclusion

Whereas treating ZrCl$_4$ with silylated iminophenols (3-Bu^t-2-(OSiMe$_3$)C$_6$H$_3$CH=N(Ar)) is not selective, TiCl$_4$ reacts cleanly to afford binuclear complexes [Ti{3-Bu^t-2-(O)C$_6$H$_3$CH=N(Ar)}Cl(μ-Cl$_3$)TiCl$_3$]. Treatment of MCl$_4$(THF)$_2$ (M = Ti or Zr) with **2a–e** provides a facile synthesis of the octahedral mono(salicylaldiminato) complexes M{3-Bu^t-2-(O)C$_6$H$_3$CH=N(Ar)}Cl$_3$(THF). The zirconium complexes are unstable in toluene solution and slowly undergo a ligand redistribution reaction, giving rise to bis(salicylaldiminato) complexes. Mono(salicylaldiminato) complexes of titanium and zirconium can be activated using MAO to give ethene polymerisation catalysts, the productivity of which is sensitive to the imine substituent. The productivities are modest compared to bis(salicylaldiminato) derived catalysts. We are currently exploring the use of these mono(salicylaldiminato) complexes as precursors to mixed ligand pre-catalysts.

Experimental

General

Syntheses were performed under nitrogen using standard Schlenk techniques. Solvents were distilled over sodium-benzophenone (diethyl ether, tetrahydrofuran), sodium (toluene), sodium–potassium alloy (light petroleum, bp 40–60 °C), or CaH$_2$ (dichloromethane). NMR solvents (CDCl$_3$, C$_6$D$_6$, C$_7$D$_8$) were dried over activated 4 Å molecular sieves and degassed by several freeze–thaw cycles. NMR spectra were recorded using a Bruker DPX300 spectrometer. Chemical shifts are reported in ppm and referenced to residual solvent resonances (^{1}H, ^{13}C); ^{19}F is relative to CFCl$_3$. Nitrogen and ethene (BOC, 99.5%) were purified by passing through columns of supported P$_2$O$_5$ with moisture indicator, and activated 4 Å molecular sieves. MAO was purchased from Witco as a 10% solution in toluene and used as received. GPC analyses were performed in-house on a Polymer Labs PL-GPC-220 or by RAPRA Technology Ltd. Elemental analyses were performed by the School analysis service. Mass spectrometry was provided by the EPSRC National Mass Spectrometry Service Centre, Swansea.

ZrCl$_4$(THF)$_2$[23] and the ligands **1a–e** were prepared following the literature procedures.[8a] Example syntheses are presented below, synthetic procedures and full characterisation data are available as ESI.†

Ligand syntheses

3-Bu^t-2-(OSiMe$_3$)C$_6$H$_3$CH=N(C$_6$H$_5$) (2a). A stirred solution of **1a** (11.9 g, 30 mmol) in light petroleum (100 cm^3) at −78 °C was treated with *n*-butyllithium (18.8 cm^3 of a 1.6 M hexane solution, 30 mmol). The resulting suspension was stirred for 2 hours at room temperature and the precipitated lithium salt isolated by filtration. The salt was dried under reduced pressure before being dissolved in tetrahydrofuran (100 cm^3). Excess trimethylsilyl chloride (20 cm^3) was added and the solution heated under reflux for 8 h. The volatiles were removed under reduced pressure. The crude product was extracted with light petroleum (40 cm^3) and crystallised at −30 °C to give large pale yellow plate-like crystals (8.9 g, 27 mmol, 91%). ^{1}H NMR (293 MHz, 293 K, CDCl$_3$): δ 8.75 (s, 1H, CH=N), 7.90 (dd, 1H, J = 5.9, 1.8 Hz, Ar–H), 7.48–7.05 (m, 7H, Ar–H), 1.45 (s, 9H, Bu^t), 0.25 (s, 9H, Si(CH$_3$)$_3$). ^{13}C NMR (75.5 MHz, 293 K, CDCl$_3$): δ 159.5 (C–O), 155.9 (C=N), 152.7, 141.5, 131.0, 129.5, 129.2, 126.6, 126.2, 122.1, 121.5 (Ar), 35.3 (*C*(CH$_3$)$_3$), 20.9 (C(*C*H$_3$)$_3$), 2.2 (Si(CH$_3$)$_3$). Anal. Found: C, 74.00; H, 8.33; N, 4.49. Calc. for C$_{20}$H$_{27}$N: C, 73.79; H, 8.36; N, 4.30%.

Complex syntheses

[Ti{3-Bu^t-2-(O)C$_6$H$_3$CH=N(C$_6$H$_5$)}Cl(μ-Cl$_3$)TiCl$_3$] (3a). A stirred solution of TiCl$_4$ (1.10 cm^3, 10 mmol) in toluene (30 cm^3) at −78 °C was treated with a solution of **2a** (1.27 g, 5 mmol) in toluene (30 cm^3). The resulting solution was then warmed to room temperature and heated under reflux for 16 h. The volatiles were removed under reduced pressure and the resulting red solid was washed with light petroleum (2 × 40 cm^3). The crude product was recrystallised from a dichloromethane–light petroleum mixture at −30 °C, affording a red microcrystalline solid (2.47 g, 4.15 mmol, 83%). ^{1}H NMR (300 MHz, 293 K, CDCl$_3$): δ 8.54 (CH=N), 7.75 (dd, 1H, J = 6.28, 1.5 Hz, Ar–H), 7.55–7.27 (m, 7H, Ar–H), 1.58 (s, 9H, C(*C*H$_3$)$_3$). ^{13}C NMR (75.5 MHz, 293 K, CDCl$_3$): δ 167.9 (C–O), 164.0 (C=N), 152.3 (Ar), 138.4, 135.2, 133.6, 129.6, 128.4, 125.7, 124.9, 124.5 (Ar), 35.6 (*C*(CH$_3$)$_3$), 29.9 (C(*C*H$_3$)$_3$). Anal. Found: C, 33.57; H, 3.41; N, 2.22; Cl, 39.01. Calc. For C$_{17}$H$_{18}$NOCl$_7$Ti$_2$: C, 34.24; H, 3.04; N, 2.35; Cl, 41.02%.

Ti{3-Bu^t-2-(O)C$_6$H$_3$CH=N(C$_6$H$_5$)}Cl$_3$(THF) (5a). A stirred solution of TiCl$_4$(THF)$_2$ (1.15 g, 3.44 mmol) in dichloromethane (20 cm^3) at −78 °C, was treated with a solution of **2a** (1.12 g, 3.45 mmol) in dichloromethane (20 cm^3). The resulting solution was allowed to warm slowly to room temperature and stirred for 16 h. The volatiles were removed under reduced pressure and the resulting red solid was washed with light petroleum (2 × 40 cm^3). The crude product was recrystallised from a dichloromethane/light petroleum solvent mixture with a drop of tetrahydrofuran added at −30 °C to give dark red, needle-shaped crystals (suitable for X-ray diffraction) (1.52 g, 3.17 mmol, 92%).[24] ^{1}H NMR (293 MHz, 293 K, CDCl$_3$): δ 8.17 (s, 1H, CH=N), 7.69–7.15 (m, 8H, Ar–H), 4.24 (m, 4H, THF), 1.72 (m, 4H, THF), 1.62 (s, 9H, Bu^t). ^{13}C NMR (75.5 MHz, 293 K, CDCl$_3$): δ 166.4 (C–O), 162.6 (C=N), 151.1, 138.8, 134.5, 133.9, 129.2, 128.3, 128.0, 125.1, 124.4 (Ar), 76.7 (THF), 35.8 (*C*(CH$_3$)$_3$), 30.1 (C(*C*H$_3$)$_3$), 25.7 (THF). Anal. Found: C, 51.49; H, 5.38; N, 2.77; Cl, 22.60. Calc. for C$_{21}$H$_{27}$NO$_2$Cl$_3$Ti: C, 52.69; H, 5.47; N, 2.93; Cl, 22.22%.

Zr{3-Bu^t-2-(O)C$_6$H$_3$CH=N(2,6-Pr$^i_2$C$_6$H$_3$)}Cl$_3$(THF) (6b). **2b** (1.36 g, 3.4 mmol) was treated with ZrCl$_4$(THF)$_2$ (1.29 g, 3.4 mmol) following a similar procedure to that for **5a**. The product was isolated in a similar fashion to **5a** giving yellow needle-shaped crystals (suitable for X-ray diffraction) (1.88 g, 3.09 mmol, 91%). ^{1}H NMR (300 MHz, 293 K, CDCl$_3$): δ 8.35 (s, 1H, CH=N), 7.71 (dd, 1H, J = 6.1, 1.6 Hz, Ar–H), 7.28–7.05 (m, Ar–H), 4.35 (m, 4H, THF), 2.37 (s 2.02 (m, 4H, THF), 1.56 (s, 9H, C(CH$_3$)$_3$), 1.32 (d, 6H, J = 6.2 Hz, CH(C*H*$_3$)$_2$), 1.04 (d, 6H, J = 6.8, CH(C*H*$_3$)$_2$).). ^{13}C NMR (75.5 MHz, 293 K, CDCl$_3$): δ 173.5 (C–O), 139.9, 138.3, 135.7, 134.5, 129.5, 128.6, 128.0, 125.7, 124.8, 123.5, 122.1 (Ar), 76.0 (THF), 35.5 (*C*(CH$_3$)$_3$), 30.1 (C(*C*H$_3$)$_3$), 28.5 (CH(*C*H$_3$)$_2$) 26.2 (CH(*C*H$_3$)$_2$), 25.8 (THF), 21.9 (*C*H(CH$_3$)$_2$). Anal. Found: C, 50.67; H, 6.19; N, 1.97; Cl, 20.61. Calc. For C$_{27}$H$_{38}$NO$_2$Cl$_3$Zr·0.5CH$_2$Cl$_2$: C, 50.92; H, 6.06; N, 2.16; Cl, 21.86%.

Ti{3-Bu^t-2-(O)C$_6$H$_3$CH=O}Cl$_3$(THF) (7). **1f** (1.6 g, 5 mmol) was treated with TiCl$_4$(THF)$_2$ (1.62 g, 5 mmol) following a similar procedure to that for **5a**. The volatiles were removed under reduced pressure and the resulting red solid was washed with light petroleum. The crude product was recrystallised from a dichloromethane–light petroleum mixture with a drop of tetrahydrofuran added and cooled to −30 °C to give red, plate-like crystals (suitable for X-ray diffraction). ^{1}H NMR (300 MHz, 293 K, CDCl$_3$): δ 9.55 (s, 1H, CH=O), 7.86 (dd, 1H, J = 7.7, 1.4 Hz, Ar–H), 7.66 (dd, 1H, J = 7.7, 1.4 Hz, Ar–H), 7.23 (t, 1H, J = 7.7 Hz, Ar–H), 4.63 (m, 4H, THF), 2.13 (m, 4H, THF), 1.55 (s, 9H, Bu^t). ^{13}C NMR (75.5 MHz, 293 K, CDCl$_3$): δ 195.4 (C=O), 139.6, 135.7, 124.8 (Ar), 77.0 (THF),

Table 8 Crystal and structure refinement data

Complex	**3b**	**4c**	**5a**	**5c**	**5e**	**6b**	**6d**	**6e**	**7**
Elemental formula	$C_{23}H_{30}Cl_7NOTi_2$	$C_{20}H_{24}Cl_3NOTi$	$C_{21}H_{26}Cl_3NO_2Ti$	$C_{24}H_{32}Cl_3NO_2Ti$	$C_{21}H_{21}Cl_3F_5NO_2Ti$	$C_{34}H_{46}Cl_3NO_2Zr$	$C_{27}H_{30}Cl_3NO_2Zr{\cdot}CH_2Cl_2$	$C_{21}H_{21}Cl_3F_5NO_2Zr$	$C_{15}H_{21}Cl_3O_3Ti$
M	680.4	448.6	478.7	520.8	568.6	698.3	683.0	612.0	403.6
Crystal system	Monoclinic	Orthorhombic	Monoclinic	Triclinic	Monoclinic	Orthorhombic	Monoclinic	Triclinic	Monoclinic
Space group (no.)	$P2_1/n$ (as 14)	$P2_12_12_1$ (19)	$P2_1/c$ (14)	$P\bar{1}$ (2)	$P2_1/c$ (14)	$Pbca$ (61)	$C2/c$ (15)	$P\bar{1}$ (2)	$P2_1/n$ (as 14)
Unit cell dimensions									
a/Å	9.880(1)	9.6328(5)	7.3850(15)	7.9120(16)	7.2176(2)	15.200(3)	25.5401(8)	7.49490(10)	10.5359(4)
b/Å	19.315(1)	14.9548(8)	31.797(6)	10.469(2)	34.4138(9)	16.336(3)	16.4653(6)	9.4703(2)	8.3775(4)
c/Å	15.511(6)	14.9811(8)	9.815(2)	15.803(3)	9.3904(2)	27.710(6)	18.4558(6)	17.3848(5)	20.2839(10)
$a/^\circ$	90	90	90	91.76(3)	90	90	90	82.6990(10)	90
$\beta/^\circ$	102.80(1)	90	102.50(3)	102.27(3)	96.5740(10)	90	129.333(2)	80.7480(10)	101.350(3)
$\gamma/^\circ$	90	90	90	94.09(3)	90	90	90	87.446(2)	90
V/Å^3	2886.4(12)	2158.1(2)	2250.1(8)	1274.4(4)	2317.10(10)	6881(2)	6003.0(4)	1207.66(5)	1755.33(14)
Z	4	4	4	2	4	8	8	2	4
D_c/Mg m^{-3}	1.566	1.381	1.413	1.357	1.630	1.348	1.511	1.683	1.527
$F(000)$	1384	928	992	544	1152	2912	2784	612	832
μ/mm^{-1}	1.220	0.777	0.753	0.671	0.775	0.582	0.838	0.845	0.952
T/K	140(1)	120(2)	140(1)	140(1)	120(2)	140(1)	120(2)	120(2)	120(2)
λ/Å	0.71073	0.6984	0.71073	0.71073	0.71073	0.71073	0.71073	0.71073	0.71073
Crystal colour, shape	Deep red, thick plate	Red block	Deep red plates	Dark red block	Red rod	Yellow needle	Yellow plate	Yellow block	Orange plate
Crystal size/mm	0.4 × 0.27 × 0.23	0.08 × 0.06 × 0.04	0.6 × 0.10 × 0.02	0.35 × 0.20 × 0.20	0.24 × 0.04 × 0.02	0.45 × 0.40 × 0.15	0.14 × 0.08 × 0.03	0.26 × 0.08 × 0.06	0.30 × 0.08 × 0.01
On the diffractometer:									
θ Range for data collection/°	1.7–25.6	1.9–30.0	1.3–25.4	1.3–25.4	3.1–27.5	2.0–25.4	3.0–27.5	3.0–27.5	3.1–27.1
Completeness (%), to θ_{max}	94.3, 25.6	99.8, 26.0	82.2, 25.4	93.1, 25.4	99.6, 27.5	83.6, 25.4	99.5, 27.5	98.9, 27.5	99.1, 27.1
Absorption correction	Not applied	Semi-empirical	Not applied	Not applied	Semi-empirical	Not applied	Semi-empirical	Semi-empirical	Semi-empirical
Total no. reflections measured (not including absences)	15791	12774	7928	7307	25995	10569	34137	22105	19393
No. of unique reflections, R_{int} for equivalents	5091, 0.043	5935, 0.029	3383, 0.268	4351, 0.044	5294, 0.086	5788, 0.019	6847, 0.091	5485, 0.097	3826, 0.123
No. of 'observed' reflections ($I > 2\sigma(I)$)	4308	5352	1907	3830	3410	4580	5756	5002	3016
Refinement:									
Data/restraints/parameters	5091/0/307	5935/0/241	3383/0/253	4351/0/283	5294/0/302	5788/0/371	6847/24/343	5485/0/302	3826/0/203
Goodness-of-fit on F^2, S	1.043	1.027	0.931	1.078	0.995	0.994	0.989	1.054	1.147
Final R indices ('observed' data) R_1, wR_2 =	0.034, 0.091	0.032, 0.077	0.088, 0.209	0.036, 0.105	0.044, 0.079	0.031, 0.079	0.056, 0.140	0.035, 0.092	0.149, 0.354
Final R indices (all data) R_1, wR_2 =	0.042, 0.094	0.038, 0.081	0.141, 0.237	0.041, 0.107	0.091, 0.091	0.042, 0.082	0.068, 0.150	0.040, 0.095	0.175, 0.364
Largest diff. peak and hole/e Å^{-3}	0.30, −0.45	0.47, −0.34	0.68, −0.72	0.34, −0.44	0.38, −0.44	0.41, −0.63	1.31, −2.02	0.62, −0.84	2.03, −0.99

For complex **4c**: Absolute structure parameter, $x = 0.06(2)$.[30]

35.7 ($C(CH_3)_3$), 30.0 ($C(CH_3)_3$), 26.1 (THF). Anal. Found: C, 42.65; H, 5.21; Cl, 25.36. Calc. For $C_{15}H_{21}O_3Cl_3Ti$: C, 44.64; H, 5.24; Cl, 26.35%.

Polymerisation procedure

A solution of MAO in toluene (50 cm^3) was saturated with ethene (1 bar) at the given temperature. Polymerisation was initiated by addition of a toluene solution of pre-catalyst into the reactor under vigorous stirring (1000 rpm). Methanol (1 cm^3) was added to terminate the polymerisation. The polymeric product was precipitated and separated from aluminium residues by addition of methanol (~300 cm^3) and 2 M HCl (~5 cm^3). The polymer was collected by filtration, washed with methanol, 2 M HCl, distilled water and again with methanol before drying until constant mass at 80 °C. Each run is the average of at least two polymerisations.

Crystal structure analyses

Crystal samples were examined in several laboratories. The crystal structure and refinement data are collected in Table 8. Intensity data for complexes **3b**, **5a**, **5c**, and **6b** were measured at UEA on a Rigaku/MSC R-Axis-IIc image-plate diffractometer equipped with a rotating anode X-ray source (Mo-Kα radiation) and graphite monochromator; complex **4c** was analysed at the Synchrotron Radiation Source at Daresbury (on a Bruker SMART 1K CCD diffractometer with radiation $\lambda = 0.6984$ Å), and data for complexes **5e**, **6d**, **6e** and **7** were recorded at the EPSRC National Crystallography Service at the University of Southampton on a Nonius KappaCCD diffractometer (with Mo-Kα radiation and graphite monochromator). The procedures for all were similar, and that for complex **3b** is described below.

From a sample of deep red plate crystals of **3b** under oil, one, *ca.* 0.4 × 0.27 × 0.23 mm, was mounted on a glass fibre and fixed in the cold nitrogen stream on the Rigaku R-Axis-IIc image-plate diffractometer. The total number of reflections recorded, to $\theta_{max} = 25.6°$, was 15791 of which 5091 were unique ($R_{int} = 0.043$); 4308 were 'observed' with $I > 2\sigma(I)$.

Data were processed using the DENZO/SCALEPACK programs.[25] The structure was determined by the direct methods routines in the SHELXS program and refined by full-matrix least-squares methods, on all unique F^2, in SHELXL).[26] The non-hydrogen atoms were refined with anisotropic displacement parameters. Hydrogen atoms were included in idealised positions and their U_{iso} values were set to ride on the U_{eq} values of the parent carbon atoms. At the conclusion of the refinement, $wR_2 = 0.094$ and $R_1 = 0.042$ for all 5091 reflections weighted $w = [\sigma^2(F_o^2) + (0.0528P)^2 + 0.724P]^{-1}$ with $P = (F_o^2 + 2F_c^2)/3$; for the 'observed' data only, $R_1 = 0.034$.[26]

In the final difference map, the highest peaks (to *ca.* 0.30 e Å^{-3}) were close to the titanium atoms.

Scattering factors for neutral atoms were taken from ref. 27. Computer programs used in this analysis have been noted above, in Table 4 of ref. 28, or in ref. 29, and were run on a Silicon Graphics Indy at the University of East Anglia, or a DEC-AlphaStation 200 4/100 in the Biological Chemistry Department, John Innes Centre.

The diffraction pattern of a crystal of compound **7** suggests the presence of a second minor crystal, whose orientation matrix could not be determined, but whose diffraction intensities may have contributed to those measured for the major crystal. This would account for the high *R* factors and large residual density for this sample. We are confident, however, that the structure is correct and that the molecular dimensions are reliable within the limits shown.

CCDC reference numbers 214921, 214922 and 250156–250162.

See http://www.rsc.org/suppdata/dt/b4/b414229b/ for crystallographic data in CIF or other electronic format.

Acknowledgements

The support of the Engineering and Physical Sciences Research Council and the University of East Anglia, together with Synchrotron Radiation Source beam-time awarded by CCLRC, are gratefully acknowledged.

References

1 (*a*) V. C. Gibson and S. K. Spitzmesser, *Chem. Rev.*, 2003, **103**, 283; (*b*) G. J. P. Britovsek, V. C. Gibson and D. F. Wass, *Angew. Chem., Int. Ed.*, 1999, **38**, 428.

2 (*a*) See, for example: S. Doherty, R. J. Errington, A. P. Jarvis, S. Collins, W. Clegg and M. R. J. Elsegood, *Organometallics*, 1998, **17**, 3408; (*b*) W.-K. Kim, M. J. Fevola, L. M. Liable-Sands, A. L. Rheingold and K. H. Theopold, *Organometallics*, 1998, **17**, 4541; (*c*) C. Morton, P. O'Shaughnessy and P. Scott, *Chem. Commun.*, 2000, 2099; (*d*) T. Matsugi, S. Matsui, S.-I. Kojoh, Y. Takagi, Y. Inoue, T. Nakano, T. Fujita and N. Kashiwa, *Macromolecules*, 2002, **35**, 4880.

3 (*a*) See, for example: E. Y. Tshuva, I. Goldberg and M. Kol, *J. Am. Chem. Soc.*, 2000, **122**, 10706; (*b*) E. Y. Tshuva, S. Groysman, I. Goldberg, M. Kol and Z. Goldschmidt, *Organometallics*, 2002, **21**, 662.

4 (*a*) K. Soga, J. R. Park and Y. Shioni, *Polym. Commun.*, 1991, **32**, 310; (*b*) M. Bochmann and S. J. Lancaster, *Organometallics*, 1993, **12**, 633; (*c*) C. Pellechia, D. Pappalardo and J. Vanbeek, *Macromol. Symp.*, 1995, **89**, 335; (*d*) Q. Y. Wang, R. Quyoum, D. J. Gillis, M. J. Tudoret, D. Jeremic, B. K. Hunter and M. C. Baird, *Organometallics*, 1996, **15**, 693.

5 (*a*) J. C. Flores, J. C. W. Chien and M. D. Rausch, *Organometallics*, 1995, **14**, 2106; (*b*) D. Liguori, R. Centore, A. Tuzi, F. Grisi, I. Sessa and A. Zambelli, *Macromolecules*, 2003, **36**, 5451.

6 M. P. Coles and P. B. Hitchcock, *Organometallics*, 2003, **22**, 5201.

7 (*a*) B. Qian, W. J. Scanlon IV, M. R. Smith III and D. H. Motry, *Organometallics*, 1999, **18**, 1693; (*b*) R. Vollmerhaus, M. Rahim, R. Tomaszewski, S. Xin, N. J. Taylor and S. Collins, *Organometallics*, 2000, **19**, 2161.

8 (*a*) S. Matsui, M. Mitani, J. Saito, Y. Tohi, H. Makio, N. Matsukawa, Y. Takagi, K. Tsuru, M. Nitabaru, T. Nakano, H. Tanaka, N. Kashiwa and T. Fujita, *J. Am. Chem. Soc.*, 2001, **123**, 6847; (*b*) S. Matsui and T. Fujita, *Catal. Today*, 2001, **66**, 63; (*c*) N. Matsukawa, S. Matsui, M. Mitani, J. Saito, K. Tsuru, N. Kashiwa and T. Fujita, *J. Mol. Catal. A.*, 2001, **169**, 99; (*d*) S. Ishii, J. Saito, M. Mitani, J. Mohri, N. Matsukawa, Y. Tohi, S. Matsui, N. Kashiwa and T. Fujita, *J. Mol. Catal. A*, 2002, **179**, 11.

9 (*a*) J. Tian, P. D. Hustad and G. W. Coates, *J. Am. Chem. Soc.*, 2001, **123**, 5134; (*b*) J. Saito, M. Mitani, J. Mohri, S. Ishii, Y. Yoshida, T. Matsugi, S. Kojoh, N. Kashiwa and T. Fujita, *Chem. Lett.*, 2001, 576; (*c*) M. Mitani, J. Mohri, Y. Yoshida, J. Saito, S. Ishii, K. Tsuru, S. Matsui, R. Furuyama, T. Nakano, H. Tanaka, S. Kojoh, T. Matsugi, N. Kashiwa and T. Fujita, *J. Am. Chem. Soc.*, 2002, **124**, 3327; (*d*) M. Mitani, R. Furuyama, J. Mohri, S. Ishii, H. Terao, T. Nakano, H. Tanaka and T. Fujita, *J. Am. Chem. Soc.*, 2003, **125**, 4293; (*e*) M. Mitani, T. Nakano and T. Fujita, *Chem. Eur. J.*, 2003, **9**, 2396.

10 D. J. Jones, V. C. Gibson, S. M. Green and P. J. Maddox, *Chem. Commun.*, 2002, 1038.

11 (*a*) T. R. Younkin, E. F. Conner, J. I. Henderson, S. K. Friedrich, R. H. Grubbs and D. A. Bansleben, *Science*, 2000, **287**, 460; (*b*) E. F. Conner, T. R. Younkin, J. I. Henderson, S. J. Hwang, R. H. Grubbs, W. P. Roberts and J. J. Litzau, *J. Polym. Sci. A. Polym. Chem.*, 2002, **40**, 2842.

12 R. K. J. Bott, D. L. Hughes, M. Schormann, M. Bochmann and S. J. Lancaster, *J. Organomet. Chem.*, 2003, **665**, 135.

13 A. F. Mason and G. W. Coates, *J. Am. Chem. Soc.*, 2004, **126**, 10798.

14 (*a*) D. A. Pennington, D. L. Hughes, M. Bochmann and S. J. Lancaster, *Dalton Trans.*, 2003, 3480; (*b*) a complementary study on mono(salicylaldiminato) complexes of titanium with aliphatic substituents on the imine nitrogen has recently been reported: D. Owiny, S. Parkin and F. T. Ladipo, *J. Organomet. Chem.*, 2003, **678**, 134.

15 (*a*) A. M. Cardoso, R. J. H. Clark and S. J. Moorhouse, *J. Chem. Soc., Dalton Trans.*, 1980, 1156; (*b*) E. C. Lund and T. Livinghouse, *Organometallics*, 1990, **9**, 2426; (*c*) M. J. Sarsfield, M. Said, M. Thornton-Pett, L. A. Gerrard and M. Bochmann, *J. Chem. Soc., Dalton Trans.*, 2001, 822, and references therein.

16 The reaction between **2d** and $TiCl_4$ gives rise to a mixture of products, which we have been unable to separate and definitively characterise.

17 F. Weller, F. Schmock and K. Dehnicke, *Z. Naturforsch., Teil B*, 1996, **51**, 1359.

18 (*a*) R. Bettenhausen, W. Milius and W. Schnick, *Chem. Eur. J.*, 1997, **3**, 1337; (*b*) See also: E. Solari, C. Floriani, A. Chiesi-Villa, C. Guastini, *J. Chem. Soc., Chem. Commun.*, 1989, 1747; (*c*) E. Solari, C. Floriani, K. Schenk, A. Chiesi-Villa, C. Rizzoli, M. Rosi and A. Sgamellotti, *Inorg. Chem.*, 1994, **33**, 2018; (*d*) Q. Feng, S. Luo, M. Olmstead, T. B. Rauchfuss and P. R. Stafford, *Chem. Mater.*, 1997, **9**, 641; (*e*) P. Kiprof, L. Jun, C. L. Renish, E. K. Kalombo and V. G. Young Junior, *J. Organomet. Chem.*, 2001, **620**, 113.

19 **X** was reported in ref. 13 without bond lengths and angles because of technical difficulties.

20 P. Bazinet, D. Wood, G. P. A. Yap and D. S. Richeson, *Inorg. Chem.*, 2003, **42**, 6225.

21 Y. Tohi, H. Makio, S. Matsui, M. Onda and T. Fujita, *Macromolecules*, 2003, **36**, 523.

22 For an example see: P. R. Woodman, N. W. Alcock, I. J. Munslow, C. J. Sanders and P. Scott, *J. Chem. Soc., Dalton Trans.*, 2000, 3340.

23 L. E. Manzer, *Inorg. Synth.*, 1982, **21**, 136.

24 Perhaps due to a tendency towards dissociation in solution, addition of a small amount of THF was found to aid recrystallisation from dichloromethane solution.

25 Z. Otwinowski and W. Minor, *Methods Enzymol.*, 1997, **276**, 307.

26 G. M. Sheldrick, *SHELX-97 – Program for crystal structure determination (SHELXS) and refinement (SHELXL)*, University of Göttingen, Germany, 1997.

27 *International Tables for X-ray Crystallography*, Kluwer Academic Publishers, Dordrecht, 1992, vol. C, pp. 500, 219 and 193.

28 S. N. Anderson, R. L. Richards and D. L. Hughes, *J. Chem. Soc., Dalton Trans.*, 1986, 245.

29 G. M. Sheldrick, *SHELXTL package, including XS (for structure determination), XL (structure refinement) and XP (molecular graphics)*, Siemens Analytical Inc., Madison, WI, USA, 1995.

30 H. D. Flack, *Acta Crystallogr., Sect. A*, 1983, **39**, 876.